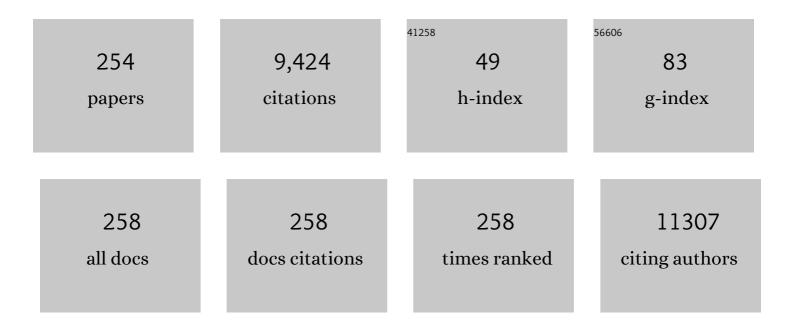
List of Publications by Year in descending order

Source: https://exaly.com/author-pdf/5569597/publications.pdf Version: 2024-02-01



PECIE COOL

#	Article	IF	CITATIONS
1	The ASTRA Toolbox: A platform for advanced algorithm development in electron tomography. Ultramicroscopy, 2015, 157, 35-47.	0.8	652
2	Verified syntheses of mesoporous materials. Microporous and Mesoporous Materials, 2009, 125, 170-223.	2.2	575
3	A Detailed Study of Thermal, Hydrothermal, and Mechanical Stabilities of a Wide Range of Surfactant Assembled Mesoporous Silicas. Chemistry of Materials, 2002, 14, 2317-2324.	3.2	325
4	Zn–Al layered double hydroxides: Synthesis, characterization and photocatalytic application. Microporous and Mesoporous Materials, 2008, 113, 296-304.	2.2	210
5	Mesoporous templated silicates: an overview of their synthesis, catalytic activation and evaluation of the stability. Advances in Colloid and Interface Science, 2003, 103, 121-147.	7.0	179
6	Plugged hexagonal templated silica: a unique micro- and mesoporous composite material with internal silica nanocapsulesElectronic supplementary information (ESI) available: Fig. S1: X-ray diffractogram of a PHTS material. Fig. S2: TEM images of SBA-15 and PHTS-2. Fig. S3: hydrothermal stabilities. See http://www.rsc.org/suppdata/cc/b2/b201424f/. Chemical Communications, 2002, , 1010-1011.	2.2	168
7	Investigation of the Morphology of the Mesoporous SBA-16 and SBA-15 Materials. Journal of Physical Chemistry B, 2006, 110, 9183-9187.	1.2	150
8	The Influence of the Alcohol Concentration on the Structural Ordering of Mesoporous Silica:Â Cosurfactant versus Cosolvent. Journal of Physical Chemistry B, 2003, 107, 10405-10411.	1.2	145
9	Catalytic performance of various mesoporous silicas modified with copper or iron oxides introduced by different ways in the selective reduction of NO by ammonia. Applied Catalysis B: Environmental, 2006, 62, 369-380.	10.8	138
10	The influence of temperature on the structural behaviour of sodium tri- and hexa-titanates and their protonated forms. Journal of Solid State Chemistry, 2005, 178, 1614-1619.	1.4	126
11	Mechanistic study of hydrocarbon formation in photocatalytic CO2 reduction over Ti-SBA-15. Journal of Catalysis, 2011, 284, 1-8.	3.1	118
12	A packed-bed DBD micro plasma reactor for CO2 dissociation: Does size matter?. Chemical Engineering Journal, 2018, 348, 557-568.	6.6	115
13	Photocatalytic removal of phenol and methylene-blue in aqueous media using TiO2@LDH clay nanocomposites. Catalysis Today, 2015, 252, 120-127.	2.2	107
14	Surfactant-Directed Synthesis of Mesoporous Titania with Nanocrystalline Anatase Walls and Remarkable Thermal Stability. Journal of Physical Chemistry B, 2004, 108, 3713-3721.	1.2	100
15	Assemblies of nanoparticles of CeO2–ZnTi-LDHs and their derived mixed oxides as novel photocatalytic systems for phenol degradation. Applied Catalysis B: Environmental, 2014, 150-151, 157-166.	10.8	99
16	Effects of Strontium on the Physicochemical Characteristics of Hydroxyapatite. Calcified Tissue International, 2004, 75, 405-415.	1.5	89
17	Synthesis of siliceous materials with micro- and mesoporosity. Microporous and Mesoporous Materials, 2007, 104, 26-38.	2.2	89
18	Anatase Formation during the Synthesis of Mesoporous Titania and Its Photocatalytic Effect. Journal of Physical Chemistry B, 2005, 109, 10081-10086.	1.2	88

#	Article	IF	CITATIONS
19	Quantitative Three-Dimensional Reconstruction of Catalyst Particles for Bamboo-like Carbon Nanotubes. Nano Letters, 2007, 7, 3669-3674.	4.5	88
20	Asymmetric dyes align inside carbon nanotubes to yield a large nonlinear optical response. Nature Nanotechnology, 2015, 10, 248-252.	15.6	88
21	Quantification of crystalline and amorphous content in porous samples from electron energy loss spectroscopy. Ultramicroscopy, 2006, 106, 630-635.	0.8	86
22	SnIV-containing layered double hydroxides as precursors for nano-sized ZnO/SnO2 photocatalysts. Applied Catalysis B: Environmental, 2008, 84, 699-705.	10.8	84
23	Modification of MCM-48-, SBA-15-, MCF-, and MSU-type Mesoporous Silicas with Transition Metal Oxides Using the Molecular Designed Dispersion Method. Journal of Physical Chemistry B, 2005, 109, 11552-11558.	1.2	83
24	Insights into phosphate adsorption behavior on structurally modified ZnAl layered double hydroxides. Applied Clay Science, 2018, 165, 234-246.	2.6	82
25	Using mesoporous silica materials to immobilise biocatalysis-enzymes. Catalysis Communications, 2005, 6, 307-311.	1.6	80
26	The relation between the synthesis of pillared clays and their resulting porosity. Applied Clay Science, 1997, 12, 43-60.	2.6	78
27	ZnO nanoparticles supported on mesoporous MCM-41 and SBA-15: a comparative physicochemical and photocatalytic study. Journal of Materials Science, 2010, 45, 5786-5794.	1.7	76
28	Fabrication of CeO2/LDHs self-assemblies with enhanced photocatalytic performance: A case study on ZnSn-LDH matrix. Applied Catalysis B: Environmental, 2015, 164, 251-260.	10.8	71
29	Combined TiO2/SiO2 mesoporous photocatalysts with location and phase controllable TiO2 nanoparticles. Applied Catalysis B: Environmental, 2009, 88, 515-524.	10.8	70
30	Preparation and characterization of SnO2 nanoparticles of enhanced thermal stability: The effect of phosphoric acid treatment on SnO2·nH2O. Colloids and Surfaces A: Physicochemical and Engineering Aspects, 2005, 268, 147-154.	2.3	68
31	Quantitative Three-Dimensional Modeling of Zeotile Through Discrete Electron Tomography. Journal of the American Chemical Society, 2009, 131, 4769-4773.	6.6	66
32	Enhanced Brönsted acidity created upon Al-grafting of porous clay heterostructures via aluminium acetylacetonate adsorption. Physical Chemistry Chemical Physics, 2000, 2, 5750-5755.	1.3	64
33	New Operando IR Technique to Study the Photocatalytic Activity and Selectivity of TiO ₂ Nanotubes in Air Purification: Influence of Temperature, UV Intensity, and VOC Concentration. Journal of Physical Chemistry C, 2012, 116, 13252-13263.	1.5	62
34	Textural property tuning of ordered mesoporous carbon obtained by glycerol conversion using SBA-15 silica as template. Carbon, 2010, 48, 1609-1618.	5.4	61
35	Plasmonic gold-embedded TiO2 thin films as photocatalytic self-cleaning coatings. Applied Catalysis B: Environmental, 2020, 267, 118654.	10.8	61
36	Structural features and photocatalytic behaviour of titania deposited within the pores of SBA-15. Applied Catalysis A: General, 2006, 312, 153-164.	2.2	60

#	Article	IF	CITATIONS
37	Threeâ€Dimensional Characterization of Helical Silver Nanochains Mediated by Protein Assemblies. Advanced Materials, 2010, 22, 2193-2197.	11.1	59
38	Threeâ€Dimensional Characterization of Nobleâ€Metal Nanoparticles and their Assemblies by Electron Tomography. Angewandte Chemie - International Edition, 2014, 53, 10600-10610.	7.2	59
39	Plugged Hexagonal Templated Silica (PHTS):Â An In-Depth Study of the Structural Characteristics. Journal of Physical Chemistry B, 2004, 108, 5263-5268.	1.2	57
40	Influence of the synthesis parameters of TiO2–SBA-15 materials on the adsorption and photodegradation of rhodamine-6G. Microporous and Mesoporous Materials, 2008, 110, 100-110.	2.2	56
41	The influence of the Ti4+ location on the formation of self-assembled nanocomposite systems based on TiO2 and Mg/Al-LDHs with photocatalytic properties. Applied Catalysis B: Environmental, 2013, 134-135, 274-285.	10.8	56
42	How process parameters and packing materials tune chemical equilibrium and kinetics in plasma-based CO2 conversion. Chemical Engineering Journal, 2019, 372, 1253-1264.	6.6	56
43	Development of photocatalytic efficient Ti-based nanotubes and nanoribbons by conventional and microwave assisted synthesis strategies. Microporous and Mesoporous Materials, 2008, 114, 401-409.	2.2	55
44	Is There Any Microporosity in Ordered Mesoporous Silicas?. Langmuir, 2009, 25, 939-943.	1.6	55
45	The benefit of glass bead supports for efficient gas phase photocatalysis: Case study of a commercial and a synthesised photocatalyst. Chemical Engineering Journal, 2011, 174, 318-325.	6.6	55
46	Characterization of Vanadium and Titanium Oxide Supported SBA-15. Journal of Physical Chemistry B, 2005, 109, 12071-12079.	1.2	54
47	SBA-15 mesoporous silica modified with metal oxides by MDD method in the role of DeNOx catalysts. Microporous and Mesoporous Materials, 2010, 127, 133-141.	2.2	54
48	PGM-free CuO/LaCoO3 nanocomposites: New opportunities for TWC application. Applied Catalysis B: Environmental, 2018, 227, 446-458.	10.8	52
49	Selective catalytic oxidation of ammonia into nitrogen over PCH modified with copper and iron species. Catalysis Today, 2006, 114, 319-325.	2.2	51
50	VOx supported SBA-15 catalysts for the oxidative dehydrogenation of ethylbenzene to styrene in the presence of N2O. Catalysis Today, 2006, 114, 307-313.	2.2	51
51	Selective catalytic reduction of NO with ammonia over porous clay heterostructures modified with copper and iron species. Catalysis Today, 2007, 119, 181-186.	2.2	51
52	A new strategy towards ultra stable mesoporous titania with nanosized anatase walls. Chemical Communications, 2003, , 1178-1179.	2.2	50
53	Catalytic decomposition and reduction of N2O over micro-mesoporous materials containing Beta zeolite nanoparticles. Applied Catalysis B: Environmental, 2014, 146, 112-122.	10.8	50
54	Structure and microstructure of nanoscale mesoporous silica spheres. Solid State Sciences, 2004, 6, 489-498.	1.5	49

#	Article	IF	CITATIONS
55	Formation of a combined micro- and mesoporous material using zeolite Beta nanoparticles. Microporous and Mesoporous Materials, 2009, 120, 29-34.	2.2	49
56	Plasmonic â€~rainbow' photocatalyst with broadband solar light response for environmental applications. Applied Catalysis B: Environmental, 2016, 188, 147-153.	10.8	49
57	Characterisation and reactivity of vanadia–titania supported SBA-15 in the SCR of NO with ammonia. Applied Catalysis B: Environmental, 2005, 61, 69-78.	10.8	48
58	Silver-polymer core-shell nanoparticles for ultrastable plasmon-enhanced photocatalysis. Applied Catalysis B: Environmental, 2017, 200, 31-38.	10.8	48
59	Novel magnetic nanocomposites containing quaternary ferrites systems Co0.5Zn0.25M0.25Fe2O4 (M = Ni, Cu, Mn, Mg) and TiO2-anatase phase as photocatalysts for wastewater remediation under solar light irradiation. Materials Science and Engineering B: Solid-State Materials for Advanced Technology, 2018. 230. 1-7.	1.7	48
60	Stabilisation of mesoporous TiO2 by different bases influencing the photocatalytic activity. Microporous and Mesoporous Materials, 2007, 99, 112-117.	2.2	47
61	Three-Dimensional Analysis of Carbon Nanotube Networks in Interconnects by Electron Tomography without Missing Wedge Artifacts. Microscopy and Microanalysis, 2010, 16, 210-217.	0.2	47
62	Self-Assembly of Pluronic F127—Silica Spherical Core–Shell Nanoparticles in Cubic Close-Packed Structures. Chemistry of Materials, 2015, 27, 5161-5169.	3.2	47
63	LDH and TiO2/LDH-type nanocomposite systems: A systematic study on structural characteristics. Microporous and Mesoporous Materials, 2015, 203, 208-215.	2.2	47
64	Acidic porous clay heterostructures: study of their cation exchange capacity. Microporous and Mesoporous Materials, 2001, 49, 83-94.	2.2	46
65	Synthesis and catalytic applications of combined zeolitic/mesoporous materials. Beilstein Journal of Nanotechnology, 2011, 2, 785-801.	1.5	44
66	Atomic layer deposition-based tuning of the pore size in mesoporous thin films studied by in situ grazing incidence small angle X-ray scattering. Nanoscale, 2014, 6, 14991-14998.	2.8	44
67	Influence of polymer matrix and adsorption onto silica materials on the migration of1±-tocopherol into 95% ethanol from active packaging. Food Additives and Contaminants, 2004, 21, 1125-1136.	2.0	43
68	The influence of the cationic ratio on the incorporation of Ti4+ in the brucite-like sheets of layered double hydroxides. Microporous and Mesoporous Materials, 2008, 111, 12-17.	2.2	43
69	Surface modified titanium dioxide using transition metals: nickel as a winning transition metal for solar light photocatalysis. Journal of Materials Chemistry A, 2018, 6, 9882-9892.	5.2	43
70	Reproducible synthesis of high quality MCM-48 by extraction and recuperation of the gemini surfactant. Physical Chemistry Chemical Physics, 2001, 3, 127-131.	1.3	42
71	Binary icosahedral clusters of hard spheres in spherical confinement. Nature Physics, 2021, 17, 128-134.	6.5	42
72	Adsorption of Hydrocarbons on Mesoporous SBA-15 and PHTS Materials. Langmuir, 2005, 21, 2447-2453.	1.6	41

#	Article	IF	CITATIONS
73	Formation mechanism of SBA-16 spheres and control of their dimensions. Microporous and Mesoporous Materials, 2006, 93, 119-124.	2.2	41
74	Epoxidation of propylene with nitrous oxide on Rb2SO4-modified iron oxide on silica catalysts. Journal of Catalysis, 2007, 247, 86-100.	3.1	40
75	In situ IR spectroscopic study to reveal the impact of the synthesis conditions of zeolite Î ² nanoparticles on the acidic properties of the resulting zeolite. Chemical Engineering Journal, 2014, 237, 372-379.	6.6	39
76	Cu@LaNiO 3 based nanocomposites in TWC applications. Applied Catalysis B: Environmental, 2017, 209, 214-227.	10.8	39
77	Photocatalytic acetaldehyde oxidation in air using spacious TiO2 films prepared by atomic layer deposition on supported carbonaceous sacrificial templates. Applied Catalysis B: Environmental, 2014, 160-161, 204-210.	10.8	37
78	Fast fabrication of hollow silica spheres with thermally stable nanoporous shells. Microporous and Mesoporous Materials, 2007, 98, 41-46.	2.2	36
79	Preparation and characterization of zirconium pillared laponite and hectorite. Microporous Materials, 1996, 6, 27-36.	1.6	35
80	Thermal transformation of polyacrylonitrile deposited on SBA-15 type silica. Journal of Thermal Analysis and Calorimetry, 2012, 110, 119-125.	2.0	35
81	Hydrothermal synthesis and formation mechanism of tetragonal barium titanate in a highly concentrated alkaline solution. Ceramics International, 2016, 42, 10967-10975.	2.3	35
82	Template extraction from porous clay heterostructures: Influence on the porosity and the hydrothermal stability of the materials. Physical Chemistry Chemical Physics, 2002, 4, 2818-2823.	1.3	34
83	Dehydrogenation of Ethylbenzene with Nitrous Oxide in the Presence of Mesoporous Silica Materials Modified with Transition Metal Oxides. Journal of Physical Chemistry A, 2005, 109, 330-336.	1.1	34
84	Multi-step loading of titania on mesoporous silica: Influence of the morphology and the porosity on the catalytic degradation of aqueous pollutants and VOCs. Applied Catalysis B: Environmental, 2008, 84, 125-132.	10.8	34
85	Plasmonic Near-Field Localization of Silver Core–Shell Nanoparticle Assemblies via Wet Chemistry Nanogap Engineering. ACS Applied Materials & Interfaces, 2017, 9, 41577-41585.	4.0	34
86	Electron Transfer and Near-Field Mechanisms in Plasmonic Gold-Nanoparticle-Modified TiO ₂ Photocatalytic Systems. ACS Applied Nano Materials, 2019, 2, 4067-4074.	2.4	34
87	Pillared Clays: Preparation, Characterization and Applications. , 1998, , 265-288.		33
88	Controlled formation of amine-templated mesostructured zirconia with remarkably high thermal stability. Journal of Materials Chemistry, 2003, 13, 3033.	6.7	33
89	Magnetism of iron-containing MCM-41 spheres. Journal of Magnetism and Magnetic Materials, 2004, 280, 31-36.	1.0	33
90	Preparation and Characterization of Vanadium Oxide Deposited on Thermally Stable Mesoporous Titania. Journal of Physical Chemistry B, 2006, 110, 948-955.	1.2	33

#	Article	IF	CITATIONS
91	Vanadium Silicalite-1 Nanoparticles Deposition onto the Mesoporous Walls of SBA-15. Mechanistic Insights from a Combined EPR and Raman Study. Journal of the American Chemical Society, 2006, 128, 8955-8963.	6.6	33
92	Unraveling Structural Information of Turkevich Synthesized Plasmonic Gold–Silver Bimetallic Nanoparticles. Small, 2019, 15, e1902791.	5.2	33
93	Photo-responsive behavior of γ-Fe2O3 NPs embedded into ZnAlFe-LDH matrices and their catalytic efficiency in wastewater remediation. Catalysis Today, 2015, 252, 7-13.	2.2	32
94	Gas phase photocatalytic spiral reactor for fast and efficient pollutant degradation. Chemical Engineering Journal, 2017, 316, 850-856.	6.6	32
95	TiOx-VOxMixed Oxides on SBA-15 Support Prepared by the Designed Dispersion of Acetylacetonate Complexes:Â Spectroscopic Study of the Reaction Mechanisms. Journal of Physical Chemistry B, 2004, 108, 3794-3800.	1.2	31
96	New TiO ₂ /MgAl-LDH Nanocomposites for the Photocatalytic Degradation of Dyes. Journal of Nanoscience and Nanotechnology, 2010, 10, 8227-8233.	0.9	31
97	Hydrothermal synthesis of a concentrated and stable dispersion of TiO2 nanoparticles. Chemical Engineering Journal, 2013, 223, 135-144.	6.6	31
98	Structure of nanoscale mesoporous silica spheres?. Journal of Physics Condensed Matter, 2003, 15, S3037-S3046.	0.7	30
99	Further investigations on the modified Stöber method for spherical MCM-41. Materials Chemistry and Physics, 2006, 97, 203-206.	2.0	30
100	SBA-15 mesoporous silica modified with rhodium by MDD method and its catalytic role for N2O decomposition reaction. Journal of Porous Materials, 2011, 18, 483-491.	1.3	30
101	Preparation of CuO/SBA-15 catalyst by the modified ammonia driven deposition precipitation method with a high thermal stability and an efficient automotive CO and hydrocarbons conversion. Applied Catalysis B: Environmental, 2018, 223, 103-115.	10.8	30
102	Fast Electron Tomography for Nanomaterials. Journal of Physical Chemistry C, 2020, 124, 27276-27286.	1.5	30
103	ZnTiLDH and the Derived Mixed Oxides as Mesoporous Nanoarchitectonics with Photocatalytic Capabilities. Journal of Inorganic and Organometallic Polymers and Materials, 2015, 25, 259-266.	1.9	29
104	Leached Natural Saponite as the Silicate Source in the Synthesis of Aluminosilicate Hexagonal Mesoporous Materials. Journal of Physical Chemistry B, 2002, 106, 4470-4476.	1.2	28
105	Benefit of Microscopic Diffusion Measurement for the Characterization of Nanoporous Materials. Chemical Engineering and Technology, 2009, 32, 1494-1511.	0.9	28
106	Mapping Composition–Selectivity Relationships of Supported Sub-10 nm Cu–Ag Nanocrystals for High-Rate CO ₂ Electroreduction. ACS Nano, 2021, 15, 14858-14872.	7.3	28
107	Catalytic Activity of MCM-48-, SBA-15-, MCF-, and MSU-Type Mesoporous Silicas Modified with Fe3+ Species in the Oxidative Dehydrogenation of Ethylbenzene in the Presence of N2O. Journal of Physical Chemistry A, 2005, 109, 9808-9815.	1.1	27
108	Integrating efficient filtration and visible-light photocatalysis by loading Ag-doped zeolite Y particles on filtration membrane of alumina nanofibers. Journal of Membrane Science, 2011, 375, 69-74.	4.1	27

#	Article	IF	CITATIONS
109	Automated discrete electron tomography– Towards routine high-fidelity reconstruction of nanomaterials. Ultramicroscopy, 2017, 175, 87-96.	0.8	27
110	Controlled Reduction of the Acid Site Density of SAPO-34 Molecular Sieve by Means of Silanation and Disilanation. Journal of Physical Chemistry B, 2003, 107, 3161-3167.	1.2	26
111	Morphology Variations of Plugged Hexagonal Templated Silica. Journal of Porous Materials, 2005, 12, 65-69.	1.3	26
112	Synthesis and structural investigations on aluminium-free Ti-Beta/SBA-15 composite. Microporous and Mesoporous Materials, 2009, 117, 458-465.	2.2	26
113	Immersion Calorimetry as a Tool To Evaluate the Catalytic Performance of Titanosilicate Materials in the Epoxidation of Cyclohexene. Langmuir, 2011, 27, 3618-3625.	1.6	26
114	Ferrite@TiO2-nanocomposites as Z-scheme photocatalysts for CO2 conversion: Insight into the correlation of the Co-Zn metal composition and the catalytic activity. Journal of CO2 Utilization, 2020, 36, 177-186.	3.3	26
115	Diffusion effects in SBA-15 and its plugged analogous by a deposition of metal–acetylacetonate complexes. Microporous and Mesoporous Materials, 2005, 85, 119-128.	2.2	25
116	Immobilisation behaviour of biomolecules in mesoporous silica materials. Catalysis Communications, 2005, 6, 591-595.	1.6	23
117	Deposition of vanadium silicalite-1 nanoparticles on SBA-15 materials. Structural and transport characteristics of SBA-VS-15. Microporous and Mesoporous Materials, 2007, 99, 14-22.	2.2	23
118	Mesoporous material formed by acidic hydrothermal assembly of silicalite-1 precursor nanoparticles in the absence of meso-templates. Microporous and Mesoporous Materials, 2008, 110, 77-85.	2.2	23
119	Preparation of hollow silica spheres with different mesostructures. Journal of Non-Crystalline Solids, 2008, 354, 826-830.	1.5	23
120	Direct spectroscopic detection of framework-incorporated vanadium in mesoporous silica materials. Physical Chemistry Chemical Physics, 2009, 11, 5823.	1.3	23
121	Synthesis of uniformly dispersed anatase nanoparticles inside mesoporous silica thin films via controlled breakup and crystallization of amorphous TiO2 deposited using atomic layer deposition. Nanoscale, 2013, 5, 5001.	2.8	23
122	Investigation on the Low-Temperature Transformations of Poly(furfuryl alcohol) Deposited on MCM-41. Langmuir, 2013, 29, 3045-3053.	1.6	23
123	Iron exchanged ZSM-5 and Y zeolites calcined at different temperatures: activity in N2O decomposition. Journal of Porous Materials, 2014, 21, 91-98.	1.3	23
124	Mechanistic Insight into the Photocatalytic Working of Fluorinated Anatase {001} Nanosheets. Journal of Physical Chemistry C, 2017, 121, 26275-26286.	1.5	23
125	Design of Ti-Beta zeolites with high Ti loading and tuning of their hydrophobic/hydrophilic character. Microporous and Mesoporous Materials, 2019, 288, 109588.	2.2	23
126	Bifunctional Nickel–Nitrogen-Doped-Carbon-Supported Copper Electrocatalyst for CO ₂ Reduction. Journal of Physical Chemistry C, 2020, 124, 1369-1381.	1.5	23

#	Article	IF	CITATIONS
127	Unraveling the Photocatalytic Activity of Multiwalled Hydrogen Trititanate and Mixed-Phase Anatase/Trititanate Nanotubes: A Combined Catalytic and EPR Study. Journal of Physical Chemistry C, 2011, 115, 2302-2313.	1.5	22
128	Mg–Al and Zn–Fe layered double hydroxides used for organic species storage and controlled release. Materials Science and Engineering C, 2013, 33, 5071-5078.	3.8	22
129	Harvesting solar light on a tandem of Pt or Pt-Ag nanoparticles on layered double hydroxides photocatalysts for p-nitrophenol degradation in water. Applied Clay Science, 2019, 182, 105250.	2.6	22
130	Self-Assembly and Diffusion of Block Copolymer Templates in SBA-15 Nanochannels. Journal of Physical Chemistry B, 2010, 114, 4223-4229.	1.2	21
131	Quaternary M0.25Cu0.25Mg0.5Fe2O4 (M=Ni, Zn, Co, Mn) ferrite oxides: Synthesis, characterization and magnetic properties. Materials Research Bulletin, 2016, 81, 63-70.	2.7	21
132	Post-synthesis deposition of V-zeolitic nanoparticles in SBA-15. Chemical Communications, 2004, , 898.	2.2	20
133	Structural Investigation of Vanadyl-Acetylacetonate-Containing Precursors of TiOxâ^'VOxMixed Oxides on SBA-15. Journal of Physical Chemistry B, 2004, 108, 19404-19412.	1.2	20
134	Rapid microwave-assisted synthesis of benzene bridged periodic mesoporous organosilicas. Journal of Materials Chemistry, 2009, 19, 3042.	6.7	20
135	The impact of framework organic functional groups on the hydrophobicity and overall stability of mesoporous silica materials. Materials Chemistry and Physics, 2012, 132, 1077-1088.	2.0	20
136	Theoretical evaluation of pillared clay adsorbents: Part I. The microporosity of Al- and Ti-pillared montmorillonite. Journal of Porous Materials, 1996, 3, 47-59.	1.3	19
137	Influence of the MCM-41 morphology on the vanadia deposition by a molecular designed dispersion method. Microporous and Mesoporous Materials, 2006, 95, 31-38.	2.2	19
138	Price tag in nanomaterials?. Journal of Nanoparticle Research, 2017, 19, 1.	0.8	19
139	CuO/La0.5Sr0.5CoO3 nanocomposites in TWC. Applied Catalysis B: Environmental, 2019, 255, 117753.	10.8	19
140	Characteristics of new composite- and classical potentiometric sensors for the determination of pharmaceutical drugs. Electrochimica Acta, 2006, 51, 5062-5069.	2.6	18
141	Gold and Silver-Catalyzed Reductive Amination of Aromatic Carboxylic Acids to Benzylic Amines. ACS Catalysis, 2021, 11, 7672-7684.	5.5	18
142	Silica-Pillared Clay Derivatives Using Aminopropyltriethoxysilane. Journal of Porous Materials, 2000, 7, 475-481.	1.3	17
143	Chemical modifications of oxide surfaces. Colloids and Surfaces A: Physicochemical and Engineering Aspects, 2001, 179, 145-150.	2.3	17
144	Removal of methyl–ethyl ketone vapour on polyacrylonitrile-derived carbon/mesoporous silica nanocomposite adsorbents. Microporous and Mesoporous Materials, 2011, 145, 65-73.	2.2	17

#	Article	IF	CITATIONS
145	Interface Pattern Engineering in Coreâ€Shell Upconverting Nanocrystals: Shedding Light on Critical Parameters and Consequences for the Photoluminescence Properties. Small, 2021, 17, e2104441.	5.2	17
146	Quantitative Information on Pore Size Distribution from the Tangents of Comparison Plots. Langmuir, 2004, 20, 10115-10122.	1.6	16
147	Nitrous Oxide Reduction with Ammonia and Methane Over Mesoporous Silica Materials Modified with Transition Metal Oxides. Journal of Porous Materials, 2005, 12, 183-191.	1.3	16
148	Copper-Containing Mixed Metal Oxides (Al, Fe, Mn) for Application in Three-Way Catalysis. Catalysts, 2020, 10, 1344.	1.6	16
149	Characterization of the Acidic Properties of Mesoporous Aluminosilicates Synthesized from Leached Saponite with Additional Aluminum Incorporation. Journal of Physical Chemistry B, 2003, 107, 8599-8606.	1.2	15
150	Physicochemical and Structural Characterization of Mesoporous Aluminosilicates Synthesized from Leached Saponite with Additional Aluminum Incorporation. Chemistry of Materials, 2003, 15, 4863-4873.	3.2	15
151	Controlling pore size and uniformity of mesoporous titania by early stage low temperature stabilization. Journal of Colloid and Interface Science, 2013, 391, 36-44.	5.0	15
152	Dynamic adsorption–desorption of methyl ethyl ketone on MCM-41 and SBA-15 decorated with thermally activated polymers. Journal of Industrial and Engineering Chemistry, 2019, 71, 465-480.	2.9	15
153	Self-assembly of aluminium-pillared clay on a gold support. Journal of Materials Chemistry, 1997, 7, 443-448.	6.7	14
154	Influence of water on the pillaring of montmorillonite with aminopropyltriethoxysilane. Physical Chemistry Chemical Physics, 1999, 1, 3703-3708.	1.3	14
155	New Insights in the Formation of Combined Zeolitic/Mesoporous Materials by using a Oneâ€Pot Templating Synthesis. European Journal of Inorganic Chemistry, 2011, 2011, 4234-4240.	1.0	14
156	Comparison between a Water-Based and a Solvent-Based Impregnation Method towards Dispersed CuO/SBA-15 Catalysts: Texture, Structure and Catalytic Performance in Automotive Exhaust Gas Abatement. Catalysts, 2016, 6, 164.	1.6	14
157	Hyperbranched polyethyleneimine towards the development of homogeneous and highly porous CuO–CeO2–SiO2 catalytic materials. Chemical Engineering Journal, 2016, 300, 343-357.	6.6	14
158	Texturing of hydrothermally synthesized BaTiO3 in a strong magnetic field by slip casting. Ceramics International, 2016, 42, 5382-5390.	2.3	14
159	Synthesis of L-serine modified benzene bridged periodic mesoporous organosilica and its catalytic performance towards aldol condensations. Microporous and Mesoporous Materials, 2017, 251, 1-8.	2.2	14
160	Acid/base treatment of Al-PILC in KCl solution. Microporous and Mesoporous Materials, 1998, 26, 185-192.	2.2	13
161	Aluminum Incorporation into MCM-48 toward the Creation of BrÃ,nsted Acidity. Journal of Physical Chemistry B, 2004, 108, 13905-13912.	1.2	13
162	Influence of the initial iron concentration on the iron-loading in MCM-41 and thermal decomposition of the supported iron complexes. Microporous and Mesoporous Materials, 2005, 79, 299-305.	2.2	13

#	Article	IF	CITATIONS
163	Growth of anatase nanoparticles inside the mesopores of SBA-15 for photocatalytic applications. Catalysis Communications, 2007, 8, 527-530.	1.6	13
164	Synthesis, structural characterization and photocatalytic activity of Ti-MCM-41 mesoporous molecular sieves. Journal of Porous Materials, 2009, 16, 109-118.	1.3	13
165	Hydrothermal synthesis of carbonate-free submicron-sized barium titanate from an amorphous precursor: Synthesis and characterization. Ceramics International, 2012, 38, 619-625.	2.3	13
166	A short solid-state synthesis leading to titanate compounds with porous structure and nanosheet morphology. Microporous and Mesoporous Materials, 2012, 147, 53-58.	2.2	13
167	Catalytic activity of cobalt grafted on ordered mesoporous silica materials in N2O decomposition and CO oxidation. Molecular Catalysis, 2017, 437, 57-72.	1.0	13
168	Multistep Loading of Titania Nanoparticles in the Mesopores of SBA-15 for Enhanced Photocatalytic Activity. Journal of Nanoscience and Nanotechnology, 2007, 7, 2511-2515.	0.9	12
169	Accessibility and Dispersion of Vanadyl Sites of Vanadium Silicate-1 Nanoparticles Deposited in SBA-15. Journal of Physical Chemistry C, 2010, 114, 12966-12975.	1.5	12
170	Zeolite Î ² nanoparticles based bimodal structures: Mechanism and tuning of the porosity and zeolitic properties. Microporous and Mesoporous Materials, 2014, 185, 204-212.	2.2	12
171	Demonstrating the Benefits and Pitfalls of Various Acidity Characterization Techniques by a Case Study on Bimodal Aluminosilicates. Langmuir, 2014, 30, 1880-1887.	1.6	12
172	Pt-doped semiconductive oxides loaded on mesoporous SBA-15 for gas sensing. Comptes Rendus Chimie, 2014, 17, 717-724.	0.2	12
173	Quantitative 3D real-space analysis of Laves phase supraparticles. Nature Communications, 2021, 12, 3980.	5.8	12
174	Mesoporous CuO/TiO2 catalysts prepared by the ammonia driven deposition precipitation method for CO preferential oxidation: Effect of metal loading. Fuel, 2022, 311, 122491.	3.4	12
175	Photocatalytic study of P25 and mesoporous titania in aqueous and gaseous environment. Catalysis Communications, 2008, 9, 1787-1792.	1.6	11
176	Olefin isomerization reactions catalyzed by ruthenium hydrides bearing Schiff base ligands. Applied Organometallic Chemistry, 2011, 25, 601-607.	1.7	11
177	Probing framework–guest interactions in phenylene-bridged periodic mesoporous organosilica using spin-probe EPR. Physical Chemistry Chemical Physics, 2014, 16, 22623-22631.	1.3	11
178	Catalytic activity of rhodium grafted on ordered mesoporous silica materials modified with aluminum in N2O decomposition. Catalysis Today, 2015, 257, 51-58.	2.2	11
179	Direct-synthesis method towards copper-containing periodic mesoporous organosilicas: detailed investigation of the copper distribution in the material. Dalton Transactions, 2015, 44, 9970-9979.	1.6	11
180	Metal loaded nanoporous silicas with tailor-made properties through hyperbranched polymer assisted templating approaches. Microporous and Mesoporous Materials, 2016, 235, 107-119.	2.2	11

#	Article	IF	CITATIONS
181	Characterization of silver-polymer core–shell nanoparticles using electron microscopy. Nanoscale, 2018, 10, 9186-9191.	2.8	11
182	ZnTi layered double hydroxides as photocatalysts for salicylic acid degradation under visible light irradiation. Applied Clay Science, 2020, 197, 105757.	2.6	11
183	Porphyrin functionalized bismuth ferrite for enhanced solar light photocatalysis. Dalton Transactions, 2020, 49, 8652-8660.	1.6	11
184	Design and applications of a home-built in situ FT-Raman spectroscopic cell. Spectrochimica Acta - Part A: Molecular and Biomolecular Spectroscopy, 2004, 60, 2969-2975.	2.0	10
185	Layered double hydroxides reconstructed in calcium glutamate aqueous solution as a complex delivery system. Applied Clay Science, 2012, 65-66, 37-42.	2.6	10
186	Experimental and statistical modeling study of low coverage gas adsorption of light alkanes on meso-microporous silica. Chemical Engineering Journal, 2012, 179, 52-62.	6.6	10
187	Tuning component enrichment in amino acid functionalized (organo)silicas. Catalysis Communications, 2017, 88, 85-89.	1.6	10
188	Physicochemical properties of ammonia-adsorbed alumina- pillared montmorillonite and structural aspects of the deammoniation process. Microporous Materials, 1994, 3, 149-158.	1.6	9
189	Preparation of barium titanate powders and colloidal processing in a strong (9.4T) magnetic field. Materials Letters, 2012, 67, 154-157.	1.3	9
190	Systematic evaluation of thermal and mechanical stability of different commercial and synthetic photocatalysts in relation to their photocatalytic activity. Microporous and Mesoporous Materials, 2012, 156, 62-72.	2.2	9
191	Influence of Synthesis Conditions on Properties of Ethane-Bridged Periodic Mesoporous Organosilica Materials as Revealed by Spin-Probe EPR. Journal of Physical Chemistry C, 2013, 117, 22723-22731.	1.5	9
192	Post-synthesis bromination of benzene bridged PMO as a way to create a high potential hybrid material. Microporous and Mesoporous Materials, 2016, 236, 244-249.	2.2	9
193	In-depth structural characterization and magnetic properties of quaternary ferrite systems Co0.5Zn0.25M0.25Fe2O4 (MÂ= Ni, Cu, Mn, Mg). Journal of Alloys and Compounds, 2020, 816, 152674.	2.8	9
194	The Potential Use of Core-Shell Structured Spheres in a Packed-Bed DBD Plasma Reactor for CO2 Conversion. Catalysts, 2020, 10, 530.	1.6	9
195	A hyperbranched polymer synthetic strategy for the efficient fixation of metal species within nanoporous structures: Application in automotive catalysis. Chemical Engineering Journal, 2021, 421, 129496.	6.6	9
196	Title is missing!. Journal of Materials Science, 1997, 5, 83-94.	1.2	8
197	The merging of silica-surfactant microspheres under hydrothermal conditions. Microporous and Mesoporous Materials, 2008, 116, 141-146.	2.2	8
198	Synthesis and Characterization of Photoreactive TiO ₂ –Carbon Nanosheet Composites. Journal of Physical Chemistry C, 2014, 118, 21031-21037.	1.5	8

#	Article	IF	CITATIONS
199	Hydrothermally synthesized BaTiO3 textured in a strong magnetic field. Ceramics International, 2015, 41, 5397-5402.	2.3	8
200	A Green Route to Copper Loaded Silica Nanoparticles Using Hyperbranched Poly(Ethylene Imine) as a Biomimetic Template: Application in Heterogeneous Catalysis. Catalysts, 2017, 7, 390.	1.6	8
201	Chemical and Structural Configuration of Pt-Doped Metal Oxide Thin Films Prepared by Atomic Layer Deposition. Chemistry of Materials, 2019, 31, 9673-9683.	3.2	8
202	Theoretical evaluation of pillared clay adsorbents: Part IV: The microporosity of Fe- and mixed Fe-Zr-pillared montmorillonite. Journal of Porous Materials, 1996, 3, 217-225.	1.3	7
203	Identification of Surfaceâ^'TiClxGroups on Silica by Raman Spectroscopy. Journal of Physical Chemistry B, 2002, 106, 6248-6250.	1.2	7
204	Novel strategies towards mesoporous titania and titania-silicate composites. Studies in Surface Science and Catalysis, 2004, 154, 789-796.	1.5	7
205	Pore REconstruction and Segmentation (PORES) method for improved porosity quantification of nanoporous materials. Ultramicroscopy, 2015, 148, 10-19.	0.8	7
206	Synthesis of aluminum-containing hierarchical mesoporous materials with columnar mesopore ordering by evaporation induced self-assembly. Microporous and Mesoporous Materials, 2016, 234, 186-195.	2.2	7
207	Balancing nanotoxicity and returns in health applications: The Prisoner's Dilemma. Toxicology, 2018, 393, 83-89.	2.0	7
208	Layer-by-Layer-Stabilized Plasmonic Gold-Silver Nanoparticles on TiO2: Towards Stable Solar Active Photocatalysts. Nanomaterials, 2021, 11, 2624.	1.9	7
209	Theoretical evaluation of pillared clay adsorbents: Part II: Differences in porosity between Al-pillared laponite and hectorite. Journal of Porous Materials, 1996, 3, 157-168.	1.3	6
210	Theoretical evaluation of pillared clay adsorbents: Part III: The total porosity and the macrostructure of Al-pillared montmorillonite and hectorite. Journal of Porous Materials, 1996, 3, 207-216.	1.3	6
211	Title is missing!. Journal of Porous Materials, 1999, 6, 323-333.	1.3	6
212	Optimisation of the surface properties of SBA-15 mesoporous silica for in-situ nanoparticle synthesis. Microporous and Mesoporous Materials, 2009, 120, 2-6.	2.2	6
213	Influence of Surfactant Concentration on the Surface Morphology of Hollow Silica Microspheres and Its Explanation. Microscopy and Microanalysis, 2011, 17, 766-771.	0.2	6
214	Smart heating profiles for the synthesis of benzene bridged periodic mesoporous organosilicas. Chemical Engineering Journal, 2011, 175, 585-591.	6.6	6
215	Microvolume TOC Analysis as Useful Tool in the Evaluation of Lab Scale Photocatalytic Processes. Catalysts, 2013, 3, 74-87.	1.6	6
216	Novel method to synthesize highly ordered ethane-bridged PMOs under mild acidic conditions: Taking advantages of phosphoric acid. Microporous and Mesoporous Materials, 2015, 207, 61-70.	2.2	6

#	Article	IF	CITATIONS
217	New insights into the mesophase transformation of ethane-bridged PMOs by the influence of different counterions under basic conditions. RSC Advances, 2015, 5, 5553-5562.	1.7	6
218	Molten-salt synthesis of tetragonal micron-sized barium titanate from a peroxo-hydroxide precursor. Advanced Powder Technology, 2017, 28, 146-154.	2.0	6
219	A simple way to design highly active titania / mesoporous silica photocatalysts. Studies in Surface Science and Catalysis, 2008, 174, 377-380.	1.5	5
220	Influence of silica forming media on the synthesis of hollow silica microspheres. Microporous and Mesoporous Materials, 2011, 138, 17-21.	2.2	5
221	Is their potential for post-synthetic brominating reactions on benzene bridged PMOs?. Microporous and Mesoporous Materials, 2012, 164, 49-55.	2.2	5
222	A framework for health-related nanomaterial grouping. Biochimica Et Biophysica Acta - General Subjects, 2017, 1861, 1478-1485.	1.1	5
223	Development of monodisperse porous microspheres of MgAl-layered double hydroxide by droplet coagulation. Powder Technology, 2021, 391, 334-343.	2.1	5
224	Nano - patents and Literature Frequency as Statistical Innovation Indicator for the use of Nano - porous Material in Three Major Sectors: Medicine, Energy and Environment. Journal of Engineering Science and Technology Review, 2016, 9, 24-35.	0.2	5
225	ZnAl layered double hydroxide based catalysts (with Cu, Mn, Ti) used as noble metal-free three-way catalysts. Applied Clay Science, 2022, 217, 106390.	2.6	5
226	Complementary use of Fourier transform laser microprobe mass spectrometry and time-of-flight static secondary ion mass spectrometry for the study of the surface adsorption of organic dyes on silicate materials. Rapid Communications in Mass Spectrometry, 2005, 19, 2809-2818.	0.7	4
227	Influence of ammonia concentration on the formation of hollow silica microspheres via polystyrene beads templating. International Journal of Materials Research, 2011, 102, 1488-1492.	0.1	4
228	New nano-architectures of mesoporous silica spheres analyzed by advanced electron microscopy. Nanoscale, 2012, 4, 1722.	2.8	4
229	Glycerol-derived Mesoporous Carbon: N2-sorption and SAXS Data Evaluation. Materials Today: Proceedings, 2015, 2, 3836-3845.	0.9	4
230	Inâ€Situ Synthesis of Bi ₂ O ₃ Nanoparticles on ZincMe (Me=Al or Cr) Layered Double Hydroxide Frameworks for Photocatalytic Oxygen Evolution from Water under Solar‣ight Activation. ChemCatChem, 2018, 10, 1598-1606.	1.8	4
231	Formation of a Ti-siliceous trimodal material with macroholes, mesopores and zeolitic features via a one-pot templating synthesis. Journal of Porous Materials, 2012, 19, 153-160.	1.3	3
232	Hierarchical materials originated from mesoporous MCF material and Beta zeolite nanoparticles – synthesis and catalytic activity in N2O decomposition. Journal of the Chinese Advanced Materials Society, 2013, 1, 48-55.	0.7	3
233	Template-free aqueous tape casting of hydrothermally synthesized barium titanate powder and the fabrication of highly {001}-{100} textured tapes. Ceramics International, 2018, 44, 9720-9727.	2.3	3

234 Pillared Clays and Porous Clay Heterostructures. , 2004, , .

#	Article	IF	CITATIONS
235	Use of Nanoscale Carbon Layers on Ag-Based Gas Diffusion Electrodes to Promote CO Production. ACS Applied Nano Materials, 2022, 5, 7723-7732.	2.4	3
236	ALO _{X} -GRAFTED POROUS CLAY HETEROSTRUCTURES (PCH) WITH COMBINED MICRO- AND MESOPOROSITY. , 2000, , .		2
237	06-P-15 - Synthesis of mesoporous aluminosilicate FSM-materials derived from synthetic and natural saponite. Studies in Surface Science and Catalysis, 2001, , 201.	1.5	2
238	Synthesis and characterization of catalytic metal semiconductor-doped siliceous materials with ordered structure for chemical sensoring. Journal of Porous Materials, 2013, 20, 1119-1128.	1.3	2
239	Effects of copper and vanadium deposition in multi-walled hydrogen trititanate and mixed-phase anatase/trititanate nanotubes. Dalton Transactions, 2013, 42, 12148.	1.6	2
240	Atomic-scale detection of individual lead clusters confined in Linde Type A zeolites. Nanoscale, 2022, 14, 9323-9330.	2.8	2
241	Molecular designed vanadia–titania supported SBA-15 for the oxidative dehydrogenation of isobutane and propane. Studies in Surface Science and Catalysis, 2005, 156, 733-740.	1.5	1
242	A facile synthesis of MCM-41 by ultrasound irradiation. Studies in Surface Science and Catalysis, 2007, 165, 169-172.	1.5	1
243	Formation of spheres and siliceous plugs in synthesizing MCF materials. Journal of Porous Materials, 2007, 14, 417-421.	1.3	1
244	The use of small volume TOC analysis as complementary, indispensable tool in the evaluation of photocatalysts at lab-scale. Studies in Surface Science and Catalysis, 2010, 175, 321-324.	1.5	1
245	MICROPOROUS PILLARED LAYERED MATERIALS FOR INORGANIC GAS AND ORGANIC VAPOR ADSORPTION. , 2000, , .		1
246	Towards Highly Loaded and Finely Dispersed CuO Catalysts via ADP: Effect of the Alumina Support. Catalysts, 2022, 12, 628.	1.6	1
247	Characterization of the Acidic Properties of Mesoporous Aluminosilicates Synthesized from Leached Saponite with Additional Aluminum Incorporation ChemInform, 2003, 34, no.	0.1	0
248	Deriving pore size distributions of solids with both micro- and mesopores from comparison plots. Studies in Surface Science and Catalysis, 2004, 154, 1456-1463.	1.5	0
249	Physicochemical and Structural Characterization of Mesoporous Aluminosilicates Synthesized from Leached Saponite with Additional Aluminum Incorporation ChemInform, 2004, 35, no.	0.1	0
250	Octane Hydroisomerization Over Hexagonal Mesoporous Aluminosilicates Synthesized from Leached Saponite. Journal of Porous Materials, 2005, 12, 35-40.	1.3	0
251	Deposition of Ti-modified aluminium-free zeolite Beta on SBA-15. Studies in Surface Science and Catalysis, 2008, , 217-220.	1.5	0
252	A scanning electron microscopy study on hollow silica microspheres: defects and influences of the synthesis composition. Journal of Sol-Gel Science and Technology, 2009, 49, 373-379.	1.1	0

#	Article	IF	CITATIONS
253	Interface Pattern Engineering in Coreâ€Shell Upconverting Nanocrystals: Shedding Light on Critical Parameters and Consequences for the Photoluminescence Properties (Small 47/2021). Small, 2021, 17, 2170246.	5.2	0
254	Efficient degradation and mineralization of diclofenac in water on ZnMe (Me: Al; Co; Ga) layered double hydroxides and derived mixed oxides as novel photocatalysts. Comptes Rendus Chimie, 2022, 25, 51-67.	0.2	0